

Formation of Millisecond Pulsars from Intermediate- and Low-Mass X-ray Binaries

Yong Shao and Xiang-Dong Li

¹*Department of Astronomy, Nanjing University, Nanjing 210093, China*

²*Key laboratory of Modern Astronomy and Astrophysics (Nanjing University), Ministry of Education, Nanjing 210093, China*

lixd@nju.edu.cn

ABSTRACT

We present a systematic study of the evolution of intermediate- and low-mass X-ray binaries consisting of an accreting neutron star of mass $1.0 - 1.8M_{\odot}$ and a donor star of mass $1.0 - 6.0M_{\odot}$. In our calculations we take into account physical processes such as unstable disk accretion, radio ejection, bump-induced detachment, and outflow from the L_2 point. Comparing the calculated results with the observations of binary radio pulsars, we report the following results. (1) The allowed parameter space for forming binary pulsars in the initial orbital period - donor mass plane increases with increasing neutron star mass. This may help explain why some MSPs with orbital periods longer than ~ 60 days seem to have less massive white dwarfs than expected. Alternatively, some of these wide binary pulsars may be formed through mass transfer driven by planet/brown dwarf-involved common envelope evolution. (2) Some of the pulsars in compact binaries might have evolved from intermediate-mass X-ray binaries with anomalous magnetic braking. (3) The equilibrium spin periods of neutron stars in low-mass X-ray binaries are in general shorter than the observed spin periods of binary pulsars by more than one order of magnitude, suggesting that either the simple equilibrium spin model does not apply, or there are other mechanisms/processes spinning down the neutron stars.

Subject headings: stars: millisecond pulsars – stars: evolution – MSPs: general

1. Introduction

Millisecond pulsars (MSPs) are neutron stars (NSs) characterized by short spin periods ($P_{\text{spin}} < 20$ ms) and weak surface magnetic fields ($B < 10^9$ G), which are often found in

binaries with a white dwarf (WD) companion. It is generally agreed that MSPs are old NSs, recycled by accretion of mass and angular momentum from the donor stars through Roche-lobe overflow (RLOF) during the previous low-mass X-ray binary (LMXB) evolution. The NS was spun up, due to mass accretion, into a MSP, while the donor evolved to be a He or CO WD (see e.g., Bhattacharya & van den Heuvel 1991; Tauris & van den Heuvel 2006, for reviews).

The stability of mass transfer in an X-ray binary depends on the ratio of the masses of the donor star and the NS, and the initial orbital period of the system. Traditionally, it was thought that, if the mass ratio is large enough ($\gtrsim 1.5$), the mass transfer is likely to be unstable, resulting in a common envelope (CE) evolution (Paczynski et al. 1976; Webbink 1984; Iben & Livio 1993), where the NS spirals into the envelope of the donor on a very short timescale ($< 10^3$ yr). More recent investigations (e.g., Tauris et al. 2000; Podsiadlowski & Rappaport 2000; Kolb et al. 2000; Podsiadlowski et al. 2002; Pfahl et al. 2003) show that X-ray binary systems with intermediate-mass (up to $\sim 5M_{\odot}$) donor stars (i.e., IMXBs) can avoid the spiral-in phase and experience rapid mass transfer on a thermal timescale, successfully evolve to become LMXBs.

For LMXBs, a CE evolution is even unavoidable if the separation of binary components is large enough, so that the donor reaches the asymptotic giant branch (AGB) phase with a deep convective envelope before RLOF (i.e. Case C RLOF). Stable mass transfer in LMXBs usually occurs on a timescale $\sim 10^8 - 10^{10}$ yr when the donor star is on the main sequence or (sub)giant branch at the onset of RLOF (i.e., Case A or B RLOF), and forming MSPs seems to be feasible in this process. It was found by Pylyser & Savonije (1988, 1989) that there exists a critical bifurcation orbital period (P_{bif}), the initial orbital period that separates the formation of converging LMXBs (which evolve with decreasing orbital periods until the donor star becomes degenerate or an ultra-compact binary is formed) from diverging LMXBs. The value of P_{bif} is found to be ~ 1 d, but depends heavily on the processes of tidal interactions and the mechanisms and efficiency of orbital angular momentum loss (Ergma et al. 1998; Podsiadlowski et al. 2002; van der Sluys, Verbunt, & Pols 2005; Ma & Li 2009).

The final products of LMXB evolution are binary pulsars. The distributions of the spin periods of the pulsars, the orbital periods and the WD masses can be used to testify the models of I/LMXB evolution. Deloye (2008) compared the theoretical expectations of I/LMXB evolution to the populations of Galactic binary pulsars. He showed that a significant population of binary pulsars with $1 \text{ d} \lesssim P_{\text{orb}} \lesssim 100 \text{ d}$ are generally consistent with being the descendants of long-period LMXBs or IMXBs. However, there remain quite a few unresolved puzzles. For example, binary pulsars with $P_{\text{orb}} \gtrsim 60 \text{ d}$ seem to have WD companions less massive than predicted by theory, as pointed out previously by Tauris & Savonije (1999),

and those with $0.1 \text{ d} \lesssim P_{\text{orb}} \lesssim 1 \text{ d}$ are inconsistent with any I/LMXB evolution.

In the previous studies on I/LMXB evolution, a canonical NS (of mass $\sim 1.3 - 1.4 M_{\odot}$) was usually adopted. This seems to be supported by the finding that the NS mass distribution is consistent with a narrow Gaussian at $1.35 \pm 0.04 M_{\odot}$ (Thorsett & Chakrabarty 1999). However, both observations (see Zhang et al. 2011; Kiziltan, Kottas, & Thorsett 2010; Schwab, Podsiadlowski, & Rappaport 2010; Özel et al. 2012, and references therein) and theories (Nomoto 1984; Timmes et al. 1996; Heger et al. 2003; Woosley & Janka 2005) suggest that the initial masses of NSs may occupy a large range, probably originating from two different mechanisms of forming NS: iron-core collapse supernovae and electron-capture supernovae. NSs in high-mass X-ray binaries (HMXBs) have experienced very little accretion because of their young ages, so their masses should be very close to those at birth. The measured masses of NSs in HMXBs range from $1.06_{-0.10}^{+0.11} M_{\odot}$ for SMC X-1 (van der Meer et al. 2007) to $1.86 \pm 0.16 M_{\odot}$ for Vela X-1 (Barziv et al. 2001; Quaintrell et al. 2003). Recently Rawls et al. (2011) present an improved method for determining the mass of NSs in eclipsing X-ray pulsar binaries and apply it to six systems. They find that the NS masses range from $0.87 \pm 0.07 M_{\odot}$ (eccentric orbit) or $1.00 \pm 0.10 M_{\odot}$ (circular orbit) for 4U1538-52 to $1.77 \pm 0.08 M_{\odot}$ for Vela X-1. So in a proper investigation, the influence of the NS masses should be included. Recent evolutionary calculations by De Vito & Benvenuto (2010) have provided evidence that the evolution of I/LMXBs depends upon the NS mass. In this work we perform systematic calculations of I/LMXB evolution and discuss the properties of the produced binary and millisecond pulsars (BMSPs), taking into account different initial NS masses. We adopt the initial donor masses to be $1.0 - 6.0 M_{\odot}$, and two different initial masses (1.0 and $1.8 M_{\odot}$) for the NS.

During the mass transfer processes, part of the transferred mass from the donor star may escape from the binary system, carrying away the orbital angular momentum. The formation of BMSPs is closely related to the mechanisms of mass and angular momentum loss, and the stability of mass transfer is also dependent on the angular momentum loss rate (Soberman et al. 1997). Generally, it is assumed that all the mass transferred from the donor will accrete onto the NS unless in a super-Eddington mass transfer phase, during which the NS will accrete at the Eddington rate ($\dot{M}_{\text{Edd}} \sim 1.5 \times 10^{-8} M_{\odot} \text{ yr}^{-1}$ for a $1.4 M_{\odot}$ NS), and the residual mass escapes from the binary system, carrying the NS’s specific orbital angular momentum. This is the so-called “isotropic reemission model”. Actually, there may also be mass loss even during the sub-Eddington mass transfer phase. For example, the accretion disk can become thermally and viscously unstable when the orbital period is larger than a critical value (van Paradijs 1996; Dubus et al. 1999), leading to limit cycle behavior of the mass transfer rate. The NS can accrete mass only during outbursts, while most matter may be ejected out of the binary systems during quiescence by the radiation and

magnetic pressure of the rapidly rotating NS (Ruderman et al. 1989; Burderi et al. 2002). In our calculations, mass loss due to super-Eddington mass transfer, radio ejection caused by an unstable disk (Burderi et al. 2002) or bump-induced detachment (D’Antona et al. 2006), and in some cases outflow from the L_2 Lagrangian point are included.

This paper is organized as follows. In Section 2 we describe the stellar evolution code and the binary model used in this paper. We present the calculated results in Section 3 and discuss their possible applications in the formation of BMSPs in Section 4, and summarize in Section 5.

2. Binary Evolutionary Calculations

2.1. The Stellar Evolution Code

All calculations were carried out with an updated version of the stellar evolution code developed by Eggleton (1971, 1972) (see also Han et al. 1994; Pols et al. 1995). We set initial solar chemical compositions (i.e., $X = 0.7$, $Y = 0.28$, and $Z = 0.02$) for the donor star, and take the ratio of the mixing length to the pressure scale height to be 2.0, and the general convective overshooting parameter to be 0.12. In our calculations, we have considered a number of binary interactions in order to follow the details of the mass transfer process, including orbital angular momentum loss due to gravitational radiation (GR), magnetic braking (MB), mass loss, and the effect of disk instability.

2.2. The Input Physics

Each of the binaries initially consists of an NS of mass M_1 ($= 1.0$ or $1.8 M_\odot$) and a zero-age main-sequence (ZAMS) donor of mass M_2 ($\sim 1.0 - 6.0 M_\odot$). The effective radius of the Roche lobe R_L of the donor is given by the following formula (Eggleton 1983),

$$R_L/a = \frac{0.49q^{-2/3}}{0.6q^{-2/3} + \ln(1 + q^{-1/3})}, \quad (1)$$

where a is the orbital separation of the binary, and $q = M_2/M_1$ is the mass ratio of the binary components. As usual we assume that tides keep the binary orbit circular (King 1988), so that the orbital angular momentum is

$$J_{\text{orb}} = \frac{M_1 M_2}{M} \Omega a^2, \quad (2)$$

where $M = M_1 + M_2$, and $\Omega = \sqrt{GM/a^3}$ is the orbital angular velocity. Logarithmic differentiation of Eq. (2) with time gives the rate of change in the orbital separation

$$\frac{\dot{a}}{a} = 2 \frac{\dot{J}_{\text{orb}}}{J_{\text{orb}}} - 2 \frac{\dot{M}_1}{M_1} - 2 \frac{\dot{M}_2}{M_2} + \frac{\dot{M}}{M}, \quad (3)$$

where the total changing rate in the orbital angular momentum is

$$\frac{\dot{J}_{\text{orb}}}{J_{\text{orb}}} = \frac{\dot{J}_{\text{GR}}}{J_{\text{orb}}} + \frac{\dot{J}_{\text{MB}}}{J_{\text{orb}}} + \frac{\dot{J}_{\text{ml}}}{J_{\text{orb}}}. \quad (4)$$

The three terms on the right-hand-side of Eq. (4) represent angular momentum loss due to GR, MB, and mass loss, respectively. The rate of angular momentum loss due to GR is calculated according to the standard formula (Landau & Lifshitz 1959; Faulkner 1971)

$$\frac{\dot{J}_{\text{GR}}}{J_{\text{orb}}} = -\frac{32G^3}{5c^5} \frac{M_1 M_2 M}{a^4}, \quad (5)$$

where G and c are the gravitational constant and the speed of light, respectively. The prescription of Verbunt & Zwaan (1981) is adopted to calculate the angular momentum loss due to MB,

$$\frac{\dot{J}_{\text{MB}}}{J_{\text{orb}}} = -3.8 \times 10^{-30} \frac{GR_2^4 M^2}{a^5 M_1} \text{ s}^{-1}, \quad (6)$$

where R_2 is the radius of the donor.

For IMXBs and wide LMXBs, the mass transfer rate $|\dot{M}_2|$ (note that $\dot{M}_2 < 0$) can be larger than the Eddington accretion rate \dot{M}_{Edd} . Thus the mass loss rate from the binary system is $\dot{M} = \dot{M}_2 + \dot{M}_{\text{Edd}}$. Here, we adopt the isotropic reemission model, assuming that the extra material leaves the binary in the form of isotropic wind from the NS, carrying off the NS's specific orbital angular momentum $j_1 = (M_2/M_1 M) J_{\text{orb}}$. The related angular momentum loss rate can be derived to be

$$\frac{\dot{J}_{\text{ml},1}}{J_{\text{orb}}} = \frac{M_2}{M_1 M} (\dot{M}_2 + \dot{M}_{\text{Edd}}). \quad (7)$$

In some cases part of the material lost from the donor star may escape the system through the L_2 Lagrangian point rather accrete onto the NS. Assuming that a fraction δ of the matter flow escapes from the binary with the specific orbital angular momentum $j_2 = a_{L_2} \Omega$, the angular momentum loss rate due to the L_2 point outflow is given by (Shao & Li 2012)

$$\frac{\dot{J}_{\text{ml},2}}{J_{\text{orb}}} = \delta \frac{a_{L_2}^2}{a^2} \frac{M \dot{M}_2}{M_1 M_2}, \quad (8)$$

where a_{L_2} is the distance between the mass center of binary and the L_2 point.

The transferred material from the donor will form an accretion disk surrounding the NS. If the effective temperature in the accretion disk is below ~ 6500 K (the hydrogen ionization temperature), the accretion disk is likely to be thermally and viscously unstable (Lasota 2001). In LMXBs irradiation from the NS may help stabilize the disk to some extent (van Paradijs 1996; King et al. 1997; Lasota 2001; Ritter 2008). The critical mass transfer rate for the disk instability is given by (Dubus et al. 1999)

$$\dot{M}_{\text{cr}} \simeq 3.2 \times 10^{-9} \left(\frac{M_1}{1.4 M_\odot} \right)^{0.5} \left(\frac{M_2}{1.0 M_\odot} \right)^{-0.2} \left(\frac{P_{\text{orb}}}{1.0 \text{ d}} \right)^{1.4} M_\odot \text{ yr}^{-1}. \quad (9)$$

If the mass transfer rate is less than \dot{M}_{cr} , the X-ray binary is assumed to become transient, experiencing short outbursts separated by long quiescent intervals. Material accumulates in the disk during the quiescent phase while the NS accretes mostly during outbursts. Define the duty cycle d ($\sim 0.001 - 0.1$, see King et al. 2003) to be the ratio of the outburst timescale to the recurrence time, the accretion rate during outbursts can be estimated as $\sim -\dot{M}_2/d$. Of course, the mass accretion rate in this case is also limited by the Eddington accretion rate.

3. Results of I/LMXB Evolution Calculations

3.1. The Initial $M_2 - P_{\text{orb}}$ Parameter Space for Successful Evolution

In Fig. 1 we outline the results of our calculations by showing the fate of the I/LMXB evolution in the initial $M_2 - P_{\text{orb}}$ diagram, similar as in Tauris et al. (2000). The left and right panels correspond to $1.0 M_\odot$ and $1.8 M_\odot$ NS, respectively. It is seen that the allowed space for successful evolution into binary pulsars (i.e., without CE evolution) is larger for $M_1 = 1.8 M_\odot$ than for $M_1 = 1.0 M_\odot$, since the lower mass ratio in the former case can stabilize mass transfer during the IMXB evolution. When $M_1 = 1.0 M_\odot$, systems with a low mass companion ($M_2 \lesssim 1.3 M_\odot$) can form binary radio pulsars with a He/CO WD companion if the initial orbital period is < 1000 d, while the lower limit of M_2 increases to $\sim 2.2 M_\odot$ when $M_1 = 1.8 M_\odot$. IMXBs can avoid spiral-in and CE evolution when $1.5 M_\odot \lesssim M_2 \lesssim 3.3 M_\odot$ and $2 \text{ d} \lesssim P_{\text{orb}} \lesssim 10 \text{ d}$ for $M_1 = 1.0 M_\odot$, and $2.4 M_\odot \lesssim M_2 \lesssim 5.5 M_\odot$ and $2 \text{ d} \lesssim P_{\text{orb}} \lesssim 40 \text{ d}$ for $M_1 = 1.8 M_\odot$, respectively. In both cases, if the initial P_{orb} is too short, the binary systems will experience either a CE phase, or become X-ray binaries with degenerate hydrogen stars (Ergma et al. 1998), possibly forming ultra-compact binaries. On the other hand, if the initial P_{orb} is too long, the donor will develop a deep convective envelope at the onset of RLOF, and a runaway mass transfer is initiated, leading to CE evolution. In Tauris et al.

(2000) systems with $M_1 = 1.3 M_\odot$, $2M_\odot \lesssim M_2 \lesssim 5M_\odot$ and $1 \text{ d} \lesssim P_{\text{orb}} \lesssim 20 \text{ d}$ can survive unstable mass transfer. These systems are right between the limiting cases presented in Fig. 1.

To see in more detail how the NS mass affects the binary evolution, we show in Fig. 2 the evolutionary paths of two IMXBs with the same donor mass $M_2 = 4 M_\odot$ and orbital period $P_{\text{orb}} = 10 \text{ d}$, but different NS mass ($1.0 M_\odot$ and $1.8 M_\odot$). At the age of $\sim 175.1 \text{ Myr}$, the donor star starts to transfer mass via RLOF. In the upper two panels with a $1.0 M_\odot$ NS, mass transfer occurs rapidly, rising up to $> 10^{-4} M_\odot \text{ yr}^{-1}$ within $\sim 10^4 \text{ yr}$. Meanwhile, the orbital period reduces to $\lesssim 4 \text{ d}$. This dynamically unstable mass transfer will result in CE evolution and probably merging of the NS and the He core of the donor. In the lower two panels with a $1.8 M_\odot$ NS, mass transfer initially proceeds at a rate of $\sim 3 \times 10^{-5} M_\odot \text{ yr}^{-1}$ for $\sim 10^5 \text{ yr}$, during which most of the hydrogen-rich envelope ($\sim 3 M_\odot$) is removed from the donor star. The mass ratio inverts during this phase, and subsequently the mass transfer rate decreases to be several $10^{-7} M_\odot \text{ yr}^{-1}$ for $\sim 10^6 \text{ yr}$. During this time the NS accretes about $0.012 M_\odot$ mass, and this is the primary process to spin up the NS. The final product is a binary consisting of a $1.815 M_\odot$ (mildly) recycled NS and a $\sim 0.6 M_\odot$ CO WD in an orbital period of $\sim 36 \text{ d}$.

3.2. The $P_{\text{orb}}^{\text{final}} - M_{\text{WD}}$ Diagram

Figure 3 shows the calculated correlation between the final orbital period $P_{\text{orb}}^{\text{final}}$ and the mass of the WD (the remnant of the donor) M_{WD} , for two different initial NS masses, $1.0 M_\odot$ (left panel) and $1.8 M_\odot$ (right panel). As mentioned above, low-mass donor stars ($M_2 \lesssim 1.3 M_\odot$ or $\lesssim 2.2 M_\odot$ for $1.0 M_\odot$ or $1.8 M_\odot$ NS, respectively) may evolve to be He WDs. However, when the mass of He is accumulated to exceed $\sim 0.4 - 0.5 M_\odot$ in the core of the donor, He flash will occur, giving rise to the formation of a CO core. The orbital period will reach $\gtrsim 10^3$ days. Intermediate-mass donors can avoid He flash due to their higher temperature, forming CO WDs with the mass $M_{\text{WD}} \gtrsim 0.33 M_\odot$. Their $P_{\text{orb}}^{\text{final}} - M_{\text{WD}}$ distribution deviates from that of the low-mass branch obviously.

3.3. Radio Ejection during the “Bump-related” Detachment?

When its hydrogen shell reaches a discontinuity in the hydrogen content at the time of the first dredge-up, a low-mass star will suffer a temporary contraction, thus producing a “bump” in the luminosity function of the red giants. D’Antona et al. (2006) suggested that

the orbital period gap ($\sim 20 - 60$ days) of BMSPs may be related to the bump-induced detachment of the donor star from its RL. If the NS has already accreted sufficient mass, it may turn on as a MSP during the detachment phase. Material transferred from the donor, once it expands again to refill its Roche lobe, may be inhibited by the pulsar’s radiation pressure and ejected at the inner lagrangian point L_1 (Ruderman et al. 1989; Burderi et al. 2002), so that no further mass accretion would occur. Similarly, this so-called “radio ejection” process may also occur in LMXBs with an unstable accretion disk (Burderi et al. 2002). In both cases the mass loss will influence the orbital evolution of the binary and the spin evolution of the NS. D’Antona et al. (2006) considered the radio ejection only during the bump-related detachment. Our calculations show that the disk instability generally appears earlier than the bump phase. Two examples are presented in Fig. 4. In the upper two panels, the binary system initially consists of a $1.0 M_\odot$ NS and a $1.0 M_\odot$ ZAMS donor star in an orbital period of 5.0 d. RLOF initiates at the age $\sim 1.186 \times 10^{10}$ yr, and the bump occurs $\sim 7 \times 10^7$ yr later, at which the donor mass has decreased to be $\sim 0.52 M_\odot$. However, the disk becomes thermally unstable when the donor mass is $\sim 0.9 M_\odot$, much earlier than the bump phase. If the NS’s spin was accelerated during the prior mass transfer, the accumulated mass in the disk during quiescence will be ejected out of the binary by the radiation pressure of the rapidly spinning NS. We find a similar situation in the case of a binary containing a $1.8 M_\odot$ NS and a $1.5 M_\odot$ donor star shown in the lower two panels. Compared with the effect of unstable disk accretion, it seems that the bump-related detachment might play a less important role in the evolution of LMXBs.

We finally note that the process of pulsar-driven mass ejection is highly uncertain, since its condition and efficiency depend on several unknown parameters (Fu & Li 2011), such as the value of the equilibrium period that a NS will reach during the mass transfer. However, as seen below, there is controversy on the estimate of the equilibrium period for NSs in LMXBs, and one should be cautious when considering the effect of radio ejection on the binary evolution.

3.4. The effect of outflow from the L_2 point

In the binary evolution the stability of mass transfer strongly depends on mass loss and related angular momentum loss. Although we have taken into account various ways for mass loss, including super-Eddington mass transfer, unstable mass transfer due to disk instability, and mass ejection due to the propeller effect and the pulsar’s radiation, the detail processes are complicated and uncertain, and simplified treatment might not reveal the realistic situation. In the following, we show an example of how outflows from the

binary systems through the L_2 point influence the evolution of mass transfer, and change the conditions of forming BMSPs.

MSP J1614–2230 is a 3.15 ms pulsar of mass $1.97 \pm 0.04 M_\odot$ (Demorest 2010). The mass of its WD companion ($0.500 \pm 0.006 M_\odot$) and the orbital period (8.7 d) were also measured accurately. Lin et al. (2011) and Tauris et al. (2011) systematically investigated the formation channels of this pulsar from an IMXB. They showed that NS this massive are not easy to produce in spite of the initially high mass of the donor star, unless they were already born as a relatively massive NS. However, Tauris et al. (2011) found that, for the system with a $1.8 M_\odot$ NS, the final orbital period will be always larger than 10 d, inconsistent with the observation of the pulsar. This conclusion will not hold if we let a small fraction δ of the transferred mass leave the system from the L_2 point (e.g., Baily et al. 1989). As an illustration, in Fig. 5 we compare the evolution of an IMXB containing a $1.8 M_\odot$ NS and a $4.5 M_\odot$ companion star in an orbit of 2.4 d, with $\delta = 0$ (upper two panels) and $\delta = 0.04$ (lower two panels), respectively. In the former case the primary angular momentum loss mechanism is the isotropic reemission around the NS during the super-Eddington accretion phase. The final system consists of a $2 M_\odot$ NS and $0.5 M_\odot$ CO WD, with a orbital period 15 d. In the latter case angular momentum loss due to the L_2 point outflow plays a role when the system evolves into an LMXB, and reduces the orbital period to ~ 8.7 days.

4. Comparison with BMSPs

4.1. The $P_{\text{orb}} - M_{\text{WD}}$ relation for low-mass BMSPs

In wide LMXBs, the donor will climb to the red-giant branch (RGB) in the HR diagram before RLOF. For low-mass stars ($< 2.3 M_\odot$) on the RGB, there is a well known relationship between the mass of the degenerate He core and the radius of the giant star, which is almost entirely independent of the mass of the hydrogen-rich envelope (Refsdal & Weigert 1971; Webbink et al. 1983). Based on this relationship, a specific correlation between the orbital period P_{orb} and the WD mass M_{WD} is obtained (Joss et al. 1987; Rappaport et al. 1995; Tauris & Savonije 1999). Comparison with the observations shows that a significant population of BMSPs with He WD companion is generally consistent with this $P_{\text{orb}} - M_{\text{WD}}$ relation. However, there seems to be a systematic deviation from the correlation for pulsars with $P_{\text{orb}} \gtrsim 60$ d, which seem to have WD companions lighter than expected (Tauris 1996).

Both systematic small values of the orbital inclination i and large NS mass can increase M_{WD} for the given observed mass functions. Since there does not seem to be any observational selection effect favoring small inclination angle i (Tauris 1996), we first examine

whether the $P_{\text{orb}} - M_{\text{WD}}$ correlation can be accounted for if the long-period BMSPs have CO WD companions. For example, Stairs et al. (2005) noticed that the Tauris & Savonije (1999) $P_{\text{orb}} - M_{\text{WD}}$ relation is incompatible at the 99.5% level with a uniform distribution of $\cos i$ if the pulsar masses are drawn from a Gaussian distribution centered on $1.35M_{\odot}$ with width $0.04M_{\odot}$, and better agreement with uniformity in $\cos i$ can be reached if the pulsar masses are large on average (e.g., $1.75 \pm 0.04M_{\odot}$). An extreme example is PSR B0820+02, which has a $0.6 M_{\odot}$ CO WD companion in a very wide orbit with $P_{\text{orb}} \simeq 1232$ d (Koester & Reimers 2000). However, in such wide binaries it is difficult for the NS to accrete enough matter (Li & Wang 1998; Tauris & Savonije 1999), and the NS must be born heavy if this interpretation is correct. In Fig. 6 we compare the relations between P_{orb} and M_{WD} in the cases that the NS has an initial mass of $1.0 M_{\odot}$ (left panel) and $1.8 M_{\odot}$ (right panel). Also plotted are binary pulsars with measured P_{orb} and M_{WD} (90% probability mass range for randomly oriented orbits) for a fixed NS mass of 1.2 and $2.0 M_{\odot}$, respectively (i.e., in each case the NS is assumed to have accreted $0.2M_{\odot}$ during the mass transfer). It is seen that some binary pulsars with $P_{\text{orb}} > 100$ d can fairly match the relation if they have massive NSs ($\sim 2M_{\odot}$) and heavy CO WDs (although in some cases small orbital inclination angles may be required), while for those with $P_{\text{orb}} < 20$ d, statistically lighter NSs ($\sim 1.2M_{\odot}$) seem to follow the relation better.

It is expected that the NS has to accrete at least a few $\sim 0.01 M_{\odot}$ mass to reach a millisecond period, but this is difficult to achieve for NSs in wide binaries (see also Liu & Chen 2011), because the mass transfer rate (which increases with increasing orbital period) is likely to be super-Eddington, and the accretion disk is likely to be unstable. In Fig. 7 we show the mass transfer rate $|\dot{M}_2|$, and the accreted mass ΔM_1 of the NS as a function of the final orbital period P_{orb} . Note that here we plot the mass transfer rate only for the stable mass transfer phase - when the accretion disk becomes unstable, we take it to be the critical value \dot{M}_{cr} at the onset of disk instability. Hence both the mass accretion rate and ΔM_1 are limited by the value of \dot{M}_{cr} : when $|\dot{M}_2|$ is less than the \dot{M}_{cr} , unstable disk accretion occurs, and the NS is assumed to accrete mass only during outbursts, and part of the matter will be ejected out of the binary systems if $|\dot{M}_2/d|$ is super-Eddington.

The left panel of Fig. 7 shows the results for a $1.0 M_{\odot}$ NS with a companion star of initial mass $M_2 = 1.0, 2.0$ and $3.0 M_{\odot}$, respectively. Generally more massive donor stars result in higher mass transfer rate, which also increases with longer orbital period P_{orb} . It is noted that (1) $|\dot{M}_2|$ is always $\gtrsim 0.1\dot{M}_{\text{Edd}}$, and (2) $\Delta M_1 \lesssim 0.3M_{\odot}$, which decreases with P_{orb} , because in wider systems the mass accretion rates (with both stable and unstable accretion disks) are more likely to be super-Eddington. The right panel is for the systems with a $1.8M_{\odot}$ NS. In the case of light companion star ($\sim 1.0M_{\odot}$), the initial orbital period should be larger than ~ 1 d, so that the critical mass transfer rate \dot{M}_{cr} is always larger than the mass transfer

rate, since \dot{M}_{cr} increases during the mass transfer process (with increasing orbit period), while the mass transfer rate $|\dot{M}_2|$ decreases all the way (Webbink et al. 1983). The accreted mass ΔM_1 by the NS is thus significantly lower than those with more massive donors. So only results with 2.0 and 3.0 M_\odot donor stars are presented, in which $\Delta M_1 \lesssim 0.35 M_\odot$, and $\dot{M}_2 \gtrsim 0.3 \dot{M}_{\text{Edd}}$.

Figure 7 shows that in general $\dot{M}_2 \gtrsim 0.1 \dot{M}_{\text{Edd}}$, and $\Delta M_1 \lesssim 0.3 M_\odot$. The distribution of the mass transfer rate is considerably higher than that ($\dot{M}_2 \sim 10^{-11} - 10^{-8} M_\odot \text{ yr}^{-1}$) obtained by Podsiadlowski et al. (2002), but more compatible with the observations of persistent LMXBs. The main reason is that we have taken into account the effect of disk instability. The ΔM_1 distribution is roughly in line with Liu & Chen (2011), who found that ΔM_1 is generally less than 0.6 M_\odot in their calculations for systems with a 1.4 M_\odot NS and a 1.0 – 2.0 M_\odot donor star. Moreover, we find that systems with initially massive NSs (1.8 M_\odot) may accrete enough mass to evolve into BMSPs with 60 d $\lesssim P_{\text{orb}} \lesssim 200$ d, while light NSs in wide binaries are more likely to be partially recycled. This seems to support our conjecture that some of the wide BMSPs might be born massive. Hopefully accurate measurements of both the pulsar and the WD masses will help settle this issue.

Löhmer et al. (2005) performed timing observations of the BMSP J1640+2224 (with an orbital period of 175 d), and constrained the WD mass to be $0.15^{+0.08}_{-0.05} M_\odot$ (1σ uncertainties), which indicates that the companion is very likely to be a low-mass He WD. In this case the massive NS + CO WD model obviously does not work, and one has to explore other possibilities. Evaporation of the companion star from a wind of relativistic particles after the pulsar turns on may decrease the companion mass significantly, but it is unlikely for wide BMSPs, since the evaporation timescale would be longer than the Hubble time (Tauris 1996).

Here we suggest another possible solution. It is interesting to note that solar-type stars are usually found to be surrounded by sub-stellar companions (usually planets and/or brown dwarfs) (Cassan et al. 2012). One may expect that in some relatively wide LMXBs the companion star had possessed substellar companion(s) in close orbits like “hot Jupiters”. When the star evolved on the giant branch it would become big enough to capture its planet/brown dwarf. The planet/brown dwarf spiraled into the envelope of the giant to initiate a CE phase. The frictional drag arising from its motion through the CE would lead to loss of its orbital angular momentum and deposit of orbital energy in the envelope. If there was enough orbital energy, the spiral-in process would expel the envelope of the giant, leaving a WD remnant (Nelemans & Tauris 1998)¹. If the initial separation between the

¹In addition, Bear & Soke (2010) suggest that the binary systems may reach stable synchronized orbits

star and the substellar object(s) is less than tens of Solar radii, the final outcome would be an under-massive WD with or without the surrounding planet/brown dwarf, depending on whether it evaporated, filled its own Roche-lobe, or survived. The discovery of a $0.053M_{\odot}$ brown dwarf in a short (0.08 d) period orbit around a $0.39M_{\odot}$ WD 0137–349 (Maxted et al. 2006) presents strong observational evidence for this interaction.

During the planet/brown dwarf-involved CE phase, the companion’s envelope expanded rapidly and filled its Roche-lobe, leading to mass transfer onto the NS. Since this phase was very short ($< 10^3$ yr), the mass transfer rate would be much higher than the Eddington limit rate for the NS, so that the NS accreted very small mass $\sim 10^{-5}M_{\odot}$ (unless the CE phase lasted much longer time). If this is the case, we have to require that *some MSPs were born this way, rather recycled during the LMXB evolution*. In the literature, this idea has already been discussed by Miller & Hamilton (2001), who showed that, the existence of the innermost, moon-sized planet in the PSR 1257+12 system suggests that the pulsar was born with approximately its current spin frequency and magnetic field. A schematic view of the formation of BMSPs with planet/brown dwarf-involved CE evolution is shown in Fig. 8.

Not only having an impact on the formation of MSPs, the substellar objects, if really exist in low-mass binaries, may also play a role in the CE evolution, especially influence the estimate of the CE efficiency parameter α_{CE} . Recently Davis et al. (2012) reconstructed the CE phase for the current sample of post-CE binaries (PCEBs) with observationally determined component masses and orbital periods. Searching for correlations between α_{CE} and the binary parameters, they found that, when the internal energy of the progenitor primary envelope is taken into account, α_{CE} decreases with increasing mass M_p of the primary (i.e., the progenitor of the WD) (see however De Marco et al. 2011), and $\alpha_{\text{CE}} \gtrsim 1$ for $1 \lesssim M_p/M_{\odot} \lesssim 2$, which seems to be in contrast with $\alpha_{\text{CE}} \sim 0.25$ derived by Ricker & Taam (2012) from numerical simulations. If there are planets/brown dwarfs around these low-mass primaries, they can contribute extra orbital energy to help expel the primary’s envelope during the RGB/AGB phase, making the CE efficiency parameter within the canonical range $0 < \alpha_{\text{CE}} < 1$.

before the onset of the CE phase. Such stable synchronized orbits allow the RGB star to lose mass prior to the onset of the CE phase. Even after the secondary enters the giant envelope, the rotational velocity is high enough to cause an enhanced mass-loss rate.

4.2. The Rebirth Periods of BMSPs

Accretion onto the NS in I/LMXBs changes both the mass and spin of the NS. The spin evolution of an accreting NS depends on the interaction between the magnetosphere and the accretion disk, as described as follows (e.g., Bhattacharya & van den Heuvel 1991): the accretion disk is truncated at the magnetospheric radius R_m , which is close to the Alfvén radius of the disk

$$R_m \simeq R_A = \left(\frac{B_s^2 R_s^6}{M_1 \sqrt{2GM_1}} \right)^{2/7},$$

where B_s and R_s are the surface magnetic field and the radius of the NS, respectively. Material is channeled to the NS at the inner radius, producing a spin-up torque. If the NS is spinning very rapidly, the disk may be truncated outside the corotation radius $R_{co} = (GM_1 P^2 / 4\pi^2)^{1/3}$, and the NS experiences a centrifugal barrier that can inhibit accretion (i.e., the so-called “propeller” effect; Illarionov & Sunyaev 1975). So the NS will eventually reach the equilibrium spin period such that $R_m = R_{co}$, or

$$P_{eq} \simeq 2.4 B_9^{6/7} R_6^{18/7} M_1^{-5/7} (\dot{M}_1 / \dot{M}_{Edd})^{-3/7} \text{ ms}, \quad (10)$$

where $B_9 = B_s / 10^9$ G, and $R_6 = R_s / 10^6$ cm. This period can be regarded as the beginning or rebirth period of recycled pulsars when accretion terminates.

The rebirth period of a MSP can be derived only when its actual spin-down time is known. Bhalerao & Kulkarni (2011) recently reported the optical discovery of the companion to the $\sim 2M_\odot$ MSP J1614–2230. The optical colors show that the $0.5M_\odot$ companion is a 2.2 Gyr old CO WD. From the age of the WD, Bhalerao & Kulkarni (2011) calculated the period of the pulsar at birth, and found that pulsar should be born with a spin close to its current value, implying that the final accretion rate was $< 10^{-2} \dot{M}_{Edd}$. This value is two orders of magnitude smaller than the estimate from theoretical calculations by Lin et al. (2011) and Tauris et al. (2011). These authors suggested that the system began as an IMXB consisting of a NS and a $\sim 4M_\odot$ main-sequence secondary, which evolved to be a CO WD with He envelope. The NS gained the most mass during the final LMXB phase lasting $\sim 5 - 10$ Myr at near-Eddington rates.

We present a systematic view on the relation between $P_{eq}/B_9^{6/7}$ and P_{orb} derived from theory and observations in Fig. 9. The solid lines outline the theoretically expected distribution of $P_{eq}/B_9^{6/7}$ ($\propto \dot{M}_1^{-3/7} M_1^{-5/7}$, here R_6 is taken to be 1) from binary evolution calculations, and the symbols represent the observations of recycled pulsars (data are taken from the ATNF Pulsar Catalogue; Manchester et al. 2005). Comparison between observations and theory shows that, except in a few cases, the observational $P_{spin}/B_9^{6/7}$ is generally larger than $P_{eq}/B_9^{6/7}$ by $\sim 1 - 2$ orders of magnitude, challenging the simple recycling the-

ory². Thus, some other mechanisms must work to produce efficient spin down torque(s) or reduce the spin-up torque due to mass accretion, if the stellar evolution models are correct. The proposed explanations can be summarized as follows.

(1) There is no definite spin equilibrium since GR may remove the angular momentum from the NS. This idea was first suggested by Papaloizou & Pringle (1978) to account for the cutoff in the spin distribution of NSs in LMXBs. The main emission mechanisms involve crustal mountains (Bildsten 1998), magnetic deformations (Cutler 2002), and unstable r -modes (Andersson 1998) in the NSs. All these processes can produce a substantial mass quadrupole moment and thus a spin-down torque due to GR. The problem with this interpretation is that, recent observational results on some millisecond X-ray pulsars have shown that the efficiency of GR induced spin-down might be too low to be responsible for balancing the spin-up process during outbursts (see Haskell & Patruno 2011; Patruno et al. 2012, and references therein). So the following models focus on modifications of the equilibrium period (Eq. [10]) that the NS will finally reach.

(2) If the NS magnetic field lines can thread the accretion disk, an extra magnetic torque will be exerted on the NS (Ghosh & Lamb 1979a), and the equilibrium period will be $\sim 1 - 3$ times that in Eq. (10) (Ghosh & Lamb 1979b; Wang 1995; Li & Wang 1996). Andersson et al. (2005) further suggested that the inner disk region may be geometrically thick and sub-Keplerian, and dominated by radiation pressure, if the mass transfer rate is above a few percent Eddington accretion rate. The coupling between the disk and magnetic field can reduce the amount of angular momentum deposited onto the NS from accretion by a factor A (the ratio of orbital angular velocity to Keplerian rotational speed in the disk, $A < 1$), compared with the case of thin disks ($A = 1$), thus a decreased spin-up torque results. Patruno et al. (2012) show that the existence of spin equilibrium as set by the disk–magnetosphere interaction is able to explain the observations of millisecond X-ray pulsars, if the spin-down torque coming from the interaction between the disk and field outside corotation is sufficiently large. However, the radial extent of the coupling between the star and the disk is highly controversial (e.g. Matt & Pudritz 2005; Ghosh 2007). Stellar and disk winds may also take away the angular momentum of the NS (Goodson et al. 1997, 1999; Ustyugova et al. 2006; Romanova et al. 2009; Zhang & Li 2010). In addition, the abrupt torque reversals observed in disk-fed X-ray pulsars Her X-1, Cen X-3, and 4U 1626–67 (Bildsten et al. 1997) suggest that current models of disk–magnetosphere interaction may have severe limitations.

²Here we assume that the current spin periods of MSPs are not far from their initial ones. This holds if their characteristic ages are longer than the cooling ages of the WDs (e.g. Lorimer et al. 1995) or the Hubble time.

(3) If Eq. (10) does apply, a decaying mass transfer rate at the end of the mass transfer process will result in relatively large rebirth period of BMSPs, provided that the \dot{M}_2 evolution time is longer than the NS spin evolution timescale (Jeffrey 1986; Ruderman et al. 1989). More recently Tauris (2012) suggested that this equilibrium will even be broken when $|\dot{M}_2|$ decreases substantially, so that the magnetospheric radius R_m becomes larger than the corotation radius R_{co} , causing the NS to enter the propeller phase. A centrifugal barrier arises to expel matter entering the magnetosphere with a braking torque

$$N \simeq \dot{M}_2 R_m^2 \Omega_K(R_m) \quad (11)$$

(where $\Omega_K(R_m)$ is the Keplerian angular velocity at R_m) to act to slow down the NS. An alternatively appropriate form for the accretion torque is (e.g. Menou et al. 1999)

$$N \simeq -\dot{M}_2 R_m^2 [\Omega_K(R_m) - \Omega_s], \quad (12)$$

where Ω_s is the angular velocity of the NS. With Eqs. (11) and (12) we recalculate the spin evolution of the NS when the donor star gradually decouples from its RL as in Tauris (2012). In Fig. 10 the blue and red lines denote the results calculated with Eqs. (11) and (12), respectively³. It is seen that the decaying mass transfer rate indeed causes an increase in the spin period, which is larger than the equilibrium period corresponding to the average mass transfer rate before decoupling. However, The calculated discrepancy seems not to be large enough to explain the deviation of the rebirth periods of BMSPs from that given by Eq. (10), especially if we adopt the torque form of Eq. (12).

(4) A decaying magnetic field may also change the rebirth period of the BMSPs, if the field decay timescale is shorter than the spin evolution timescale, so that the final spin period deviates from the equilibrium period. During the decay of the NS magnetic field induced by accretion, the spin-up timescale increases as R_m decreases because the accreting matter carries less specific angular momentum, while the field decay timescale decreases as R_m decreases (field decay stops when $R_m = R_s$), resulting in a significant departure from the spin-up line (Burderi et al. 1996; Konar & Bhattacharya 1999).

(5) The rebirth periods of BMSPs may be related to the long-term spin equilibrium with varying mass accretion rate. A significant fraction of LMXBs are likely to be transient systems subject to disk instability (Coriat et al. 2012). For example, an NS LMXB in a 10 hr orbit would be transient if the average mass transfer rate is lower than $\sim 10^{17} \text{ gs}^{-1}$. In addition, in narrow LMXBs, X-ray irradiation of the donor star could destabilize the mass

³The discontinuity at the point where the two lines meets is due to the fact that we use Eq. (12) to calculate the spin evolution even before the propeller phase in both cases.

transfer, and lead to mass transfer cycles (Hameury et al. 1993) - mass transfer is spasmodic with phases of high mass transfer driven by the thermal expansion of the convective envelope of the irradiated donor alternating with phases with low or no mass transfer, during which the donor readjusts towards thermal equilibrium of the un-irradiated star. The final spin period is thus determined by the spin-up during outbursts/high mass transfer phase balanced by the spin-down during quiescence/low mass transfer phase, which may be considerably longer than that attained via stable mass accretion (Li et al. 1998; Patruno et al. 2012).

Currently our knowledge about the evolution of LMXBs and accretion disks is not sufficient to tell which one is the dominant factor in determining the rebirth periods of BMSPs. Perhaps they are influenced by a combination of (at least some of) the above-mentioned mechanisms.

4.3. Origin of Intermediate-Mass BMSPs with $P_{\text{orb}} \lesssim 1$ d

It is well known that a large fraction of IMXBs will produce binary pulsars with a CO WD companion. As shown in **Fig. 3**, the orbital periods of these intermediate-mass binary pulsars (IMBPs) are generally $> \sim 3 - 6$ d. This leaves the puzzle that the binary pulsars with $P_{\text{orb}} \lesssim 1$ d and a CO WD companion are hard to explain reasonably in any binary population (Deloye 2008). In Table 1 we list the parameters of IMBPs with $P_{\text{orb}} \lesssim 1$ d. Except PSR B0655+64, other pulsars share the characteristics of rapid spin and low magnetic field.

The small orbital periods combined with massive WDs suggest that this type of systems may have evolved through a CE and spiral-in phase (van den Heuvel & Taam 1984). Similar to that of the Double NSs, their direct progenitors could be binaries consisting of a He star and a NS star in a close and circular orbit, as a result of spiral-in of a wide binary in late Case B or Case C mass transfer. The core of the companion was a He star which could already have gone through quite some He burning. After the spiral-in one then had a He star with already CO in its core. During He-shell burning, the envelopes of the He stars, if their masses are $< 3.5 M_{\odot}$, will expand and slowly transfer mass to the NS, which will have caused the spin-up and recycling of the NS. This interpretation seem to be responsible for PSR B0655+64 (van den Heuvel & Taam 1984), which has the longest spin period (195.6 ms) and highest magnetic field ($B \sim 10^{10}$ G) among the pulsars in Table 1, implying that it has been partially recycled with little mass accreted. For other pulsars, the short periods and low magnetic fields ($B \sim 10^8$ G) require that at least some $10^{-2} M_{\odot}$ material has been accreted by the NSs. Recently Chen et al. (2011) presented the detailed binary evolution calculation for a binary consisting of a NS (of mass $1.3 M_{\odot}$) and a low-mass He star (of mass

$1.0 M_{\odot}$) with an initial orbital period of 0.5 d. They showed that the mass transfer seems to be able to spin up the NS’s spin to milliseconds, producing BMSPs like PSR J1802–2124, which has a short orbital period $P_{\text{orb}} \lesssim 1$ d.

Another possible way to form compact IMBPs invokes evolution of IMXBs with anomalous MB. Traditionally MB is thought to work in low-mass, main-sequence stars. However, There are many intermediate-mass stars which have anomalously high magnetic fields ($\gtrsim 100$ G), i.e., Ap/Bp stars. In IMXBs, the irradiation-driven stellar wind from the surface of the Ap/Bp donor star by the NSs may couple with the high magnetic fields, resulting in angular momentum loss at a rate (Justham et al. 2006),

$$\dot{J}_{\text{MB}} = -B_2 \left(\frac{\psi \dot{M}_2 M_1}{a^3} \right)^{1/2} \left(\frac{R_2^{15}}{GM_2^3} \right)^{1/4}, \quad (13)$$

where B_2 is the magnetic field strength at the surface of the donor star, and ψ is a parameter with typical value $\psi/c^2 \sim 10^{-6}$, combining the wind-driving energy conversion efficiency and irradiation geometry. Justham et al. (2006) explored the effect of anomalous MB in the formation of compact BH LMXBs, in which the orbital energy of the companion star, if of low-mass initially, would be unable to expel the envelope of the BH progenitor. For the black hole LMXB XTE J1118+480, González Hernández et al. (2012) measured a decay rate of the orbital period $\dot{P}_{\text{orb}} = -1.83 \pm 0.66 \text{ ms yr}^{-1}$. This value is much larger than predicted by most conventional MB and mass loss models for the binary parameters of XTE J1118+480, unless the companion star has a surface magnetic field $B_2 \geq 10 - 20 \text{ kG}$ to enhance MB.

In Fig. 11 we show the evolution of a binary initially consisting of a $1.8 M_{\odot}$ NS and a $3.5 M_{\odot}$ donor with $P_{\text{orb}} \simeq 2.5$ d. We assume that the donor possesses a surface magnetic field $B_2 = 500$ G. RLOF starts at the age $\sim 2.4 \times 10^8$ yr with a mass transfer rate $\sim 10^{-5} M_{\odot} \text{ yr}^{-1}$. Because the donor is initially more massive than the NS, the orbital period decreases rapidly. Most of the transferred mass is assumed to be ejected out of the binary in the vicinity of the NS, taking away both mass and orbital angular momentum. The orbit starts to widen when $M_2 \sim 2 M_{\odot}$. When the donor mass decreases to be $\sim 0.8 M_{\odot}$, the mass transfer rate reduces to be $< 10^{-7} M_{\odot} \text{ yr}^{-1}$. In the subsequent $\sim 8 \times 10^7$ yr, MB begins to dominate the evolution. The orbital period keeps decreasing, the NS accretes most mass in this phase and is spun up to milliseconds. The final outcome is a tight binary system consisting of a $\sim 2.1 M_{\odot}$ NS and a $\sim 0.5 M_{\odot}$ WD with $P_{\text{orb}} \sim 0.4$ d.

The anomalous MB model will not work if the NS is initially of low-mass ($\sim 1 M_{\odot}$), since the allowed parameter space for forming binary pulsars will be very small (see Fig. 1). Additionally we note that models involving accretion-induced collapse of an ONeMg WD cannot account for the P_{orb} distribution of these BMSPs (Sutantyo & Li 2000).

5. Summary

This work is motivated by the fact the evolution of I/LMXBs with canonical NSs seems to meet difficulties in explaining some of the observational characteristics of BMSPs, and the measurements of the NS masses indicate a wide distribution $\sim 1 - 1.8 M_{\odot}$. We have performed numerical calculations of the evolution of I/LMXBs consisting of a 1.0 or $1.8 M_{\odot}$ NS and a $1.0 - 6.0 M_{\odot}$ donor star, to investigate its dependence on the initial NS mass, and the properties of the descendent BMSPs. The main results can be summarized as follows.

1. The allowed parameter space in the initial $P_{\text{orb}} - M_2$ diagram for forming recycled pulsars increases with increasing NS mass. This may help explain the formation of BMSPs with $P_{\text{orb}} \gtrsim 60$ d and their distribution in the $P_{\text{orb}} - M_{\text{WD}}$ diagram. Alternatively, some of these wide binary pulsars may be formed through mass transfer driven by planet/brown dwarf-involved CE evolution.

2. The equilibrium spin periods P_{eq} of accreting NSs in LMXBs derived from the standard magnetosphere-accretion disk interaction model are in general shorter than the observed spin periods of BMSPs by more than one order of magnitude. This implies that either the simple equilibrium spin model does not apply for the spin evolution in accreting NSs, or there are other mechanisms/processes to spin down the NSs when forming BMSPs.

3. Some of the compact IMBPs might have evolved from IMXBs in which the companion star were strongly magnetized Ap/Bp stars with enhanced MB.

4. Our calculations doubt the suggestion that the orbital period gap ($\sim 20 - 60$ d) of BMSPs is related to the occurrence of the bump-related detached phase in the LMXB evolution, since the accretion disk would become unstable at earlier time.

We are grateful to Ed van den Heuvel for helpful discussions and the referee for constructive comments. This work was supported by the Natural Science Foundation of China under grant number 11133001, the National Basic Research Program of China (973 Program 2009CB824800), and the Qinglan project of Jiangsu Province.

REFERENCES

- Andersson, N. 1998, *ApJ*, 502, 708
- Andersson, N., Glampedakis, K., Haskell, B., & Watts, A. L. 2005, *MNRAS*, 361, 1153
- Bailyn, C. D., Garcia, M. R., & Grindlay, J. E. 1989, *ApJ*, 344, 786

- Barziv, O., Kaper, L., Van Kerkwijk, M. H., Telting, J. H., & van Paradijs, J. 2001, *A&A*, 377, 925
- Bear, E. & Soker, N. 2010, *New Astronomy*, 15, 483
- Bhalerao, V. B. & Kulkarni, S. R. 2011, *ApJ*, 737, L1
- Bhattacharya, D. & van den Heuvel, E. P. J. 1991, *Phys. Rev.*, 203, 1
- Bildsten, L. 1998, *ApJ*, 501, L89
- Bildsten, L., Chakrabarty, D., Chiu, J., Finger, M. H., & Koh, D. T. et al. 1997, *ApJS*, 113, 367
- Burderi, L., D’Antona, F., & Burgay, M. 2002, *ApJ*, 574, 325
- Burderi, L., King, A. R., & Wynn, G. A. 1996, *MNRAS*, 283, L63
- Cassan, A., Kubas, D., Beaulieu, J.-P., Dominik, M., Horne, K. et al. 2012, *Nature*, 481, 167
- Chen, W.-C., Li, X.-D., & Xu, R.-X., 2011, *A&A*, 530, 104
- Coriat, M., Fender, R. P., & Dubus, G. 2012, arXiv:1205.5038
- Cutler C., 2002, *Phys. Rev. D*, 66, 084025
- D’Antona F., Ventura P., Burderi L., Di Salvo T., & Lavagetto G. , et al. 2006, *ApJ*, 640, 950
- Davis, P. J., Kolb, U., & Knigge, C. 2012, *MNRAS*, 419, 287
- Deloye C. J. 2008, in *40 YEARS OF PULSARS: Millisecond Pulsars, Magnetars and More.* AIP Conference Proceedings, Eds. C. Bassa, Z. Wang, A. Cumming, & V. M. Kaspi, Vol. 983, p. 501
- De Marco, O., Passy, J., Moe, M., Herwig, F., & Mac Low, M. et al. 2011, *MNRAS*, 411, 2277
- Demorest P. B., Pennucci T., Ransom S. M., Roberts M. S. E., & Hessels J. W. T., 2010, *Nature*, 467, 1081
- De Vito, M. A. & Benvenuto, O. G., 2010, *MNRAS*, 401, 2552
- Dubus, G., Lasota, J.-P., Hameury, J.-M., & Charles, P. 1999, *MNRAS*, 303, 139

- Eggleton, P. P. 1971, MNRAS, 151, 351
- Eggleton, P. P. 1972, MNRAS, 156, 361
- Eggleton, P. P. 1983, ApJ, 268, 368
- Ergma, E., Sarna, M. J., & Antipova, J. 1998, MNRAS, 300, 352
- Faulkner, J. 1971, ApJ, 170, L99
- Ferdman, R. D., Stairs, I. H., Kramer, M., McLaughlin, M. A., & Lorimer, D. R. et al. 2010, ApJ, 711, 764
- Fu, L. & Li, X.-D. 2011, RAA, 11, 1457
- Ghosh, P. 2007, Rotation and Accretion Powered Pulsars (World Scientific, London), p. 772
- Ghosh, P. & Lamb, F. K. 1979a, ApJ, 232, 259
- Ghosh, P. & Lamb, F. K. 1979b, ApJ, 234, 296
- González Hernández, J., Rafael Rebolo, R. & Casares, J. 2012, ApJ, 744L, 25
- Goodson, A. P., Böhm, K. H., & Winglee, R. M. 1999, ApJ, 524, 142
- Goodson, A. P., Winglee, R. M., & Böhm, K. H. 1997, ApJ, 489, 199
- Hameury, J. M., King, A. R., Lasota, J. P., & Raison, F. 1993, A&A, 277, 81
- Han, Z., Podsiadlowski, P., & Eggleton, P.P, 1994, MNRAS, 270, 121
- Haskell, B. & Patruno, A. 2011, ApJ, 738, 14
- Heger, A., Fryer, C. L., Woosley, S. E., Langer, N. & Hartmann, D. H. 2003, ApJ, 591, 288
- Iben, Jr. & Livio, M., 1993, PASP, 105, 1373
- Jeffrey, L. C. 1986, Nature, 319, 384
- Illarionov, A. F. & Sunyaev, R. A. 1975, A&A, 39, 185
- Joss, P. C., Rappaport, S. A., & Lewis, W. 1987, ApJ, 319, 180
- Justham, S., Rappaport, S., & Podsiadlowski, P. 2006, MNRAS, 366, 1415
- King, A. R. 1988, QJRAS, 29, 1

- King, A. R., Kolb, U., & Sienkiewicz, E. 1997, *ApJ*, 488, 89
- King A. R., Rolfe D. J., Kolb U., & Sshenker K., 2003, *MNRAS*, 341, L35
- Kiziltan, B., Kottas, A., & Thorsett, S. E. 2010, arXiv:1011.4291
- Koester, D. & Reimers, D. 2000, *A&A*, 364, L66
- Kolb, U., Davies, M. B., King, A., & Ritter, H. 2000, *MNRAS*, 317, 438
- Konar, S. & Bhattacharya, D. 1999, *MNRAS*, 303, 588
- Landau, L. D. & Lifshitz, E. M. 1959, *The Classical Theory of Fields* (Oxford: Pergamon Press)
- Lasota, J.-P. 2001, *New Astron. Rev.*, 45, 449
- Li, X.-D., van den Heuvel, E. P. J., & Wang, Z.-R. 1998, *ApJ*, 497, 865
- Li, X.-D. & Wang, Z.-R. 1996, *A&A*, 307, L5
- Li, X.-D. & Wang, Z.-R. 1998, *ApJ*, 500, 935
- Lin, J., Rappaport, S., Podsiadlowski, P., Nelson, L., Paxton, B., & Todorov, P. 2011, *ApJ*, 732, 70
- Liu, W.-M. & Chen, W.-C, 2011, *MNRAS*, 416, 2285
- Löhmer, O., Lewandowski, W., Wolszczan, A., & Wielebinski, R. 2005, *ApJ*, 621, 388
- Lorimer, D. R., Lyne, A. G., Festin, L., & Nicastro, L. 1995, *Nature*, 376, 393
- Ma, B. & Li, X.-D. 2009, *ApJ*, 691, 1611
- Manchester, R. N., Hobbs, G. B., Teoh, A., & Hobbs, M. 2005, *AJ*, 129, 1993
- Matt, S. & Pudritz, R. E. 2005, *ApJ*, 632, L135
- Maxted, R. F. L., Napiwotzki, R., Dobbie, P. D., & Burleigh, M. R. 2006, *Nature*, 442, 543
- Menou, K., Esin, A. A., Narayan, R., Garcia, M. R., Lasota, J.-P., & McClintock, J. E. 1999, *ApJ*, 520, 276
- Miller, M. C. & Hamilton, D. P. 2001, *ApJ*, 550, 863
- Nelemans, G. & Tauris, T. M. 1998, *A&A*, 335, L85

- Nomoto, K. 1984, *ApJ*, 277, 791
- Özel, F., Psaltis, D., Narayan, R., & Villarreal, A. S. 2012, *ApJ* submitted (arXiv:1201.1006)
- Paczynski, B. 1976, In *Structure and Evolution in Close Binary Systems*. Proc. IAU Symp. 73, Eds., Eggleton, P. P., Mitton, S., Whealan, J. (Reidel, Dordrecht), p. 75
- Papaloizou, J. & Pringle, J. E. 1978, *MNRAS*, 184, 501
- Patruno, A., Haskell, B., & D'Angelo, C. 2012, *ApJ*, 746, 9
- Pfahl, E., Rappaport, S., & Podsiadlowski, P. 2003, *ApJ*, 597, 1036
- Podsiadlowski, Ph. & Rappaport, S. 2000, *ApJ*, 529, 946
- Podsiadlowski, Ph., Rappaport, S., & Pfahl, E. D. 2002, *ApJ*, 565, 1107
- Pols, O.R., Tout, C.A., Eggleton, P.P., & Han Z., 1995, *MNRAS*, 274, 964
- Pylyser, E. & Savonije, G. J. 1988, *A&A*, 191, 57
- Pylyser, E. & Savonije, G. J. 1989, *A&A*, 208, 52
- Quaintrell, H., Norton, A. J., Ash, T. D. C., Roche, P., & Willems, B. et al. 2003, *A&A*, 401, 313
- Rappaport, S.A., Podsiadlowski, P., Joss, P.C., Di Stefano, R., & Han, Z. 1995, *MNRAS*, 273, 731
- Rawls, M. L., Orosz, J. A., McClintock, J. E., Torres, M. A. P., & Bailyn, C. D. et al. 2011, *ApJ*, 730, 25
- Refsdal, S. & Weigert, A. 1971, *A&A*, 13, 367
- Ricker, P. M. & Taam, R. E. 2012, *ApJ*, 746, 74
- Ritter, A. 2008, *New A Rev.*, 51, 869
- Romanova, M. M., Ustyugova, G. V., Koldoba, A. V., & Lovelace, R. V. E. 2009, *MNRAS*, 399, 1802
- Ruderman, M., Shaham, J., & Tavani, M. 1989, *ApJ*, 336, 507
- Schwab, J., Podsiadlowski, P., & Rappaport, S. 2010, *ApJ*, 719, 722
- Shao, Y. & Li, X.-D. 2012, *ApJ*, 745, 165

- Soberman, G. E., Phinney, E. S., & van den Heuvel, E. P. J. 1997, *A&A*, 327, 620
- Stairs, I. H., Faulkner, A. J., Lyne, A. G., Kramer, M., & Lorimer, D. R. et al. 2005, *ApJ*, 632,1060
- Sutantyo, W. & Li, X.-D. 2000, *A&A*, 360, 633
- Tauris, T. M. 1996. *A&A*, 315, 453
- Tauris, T. M. 2012, *Science*, 335, 561
- Tauris, T. M., Langer N., & Kramer M. 2011, *MNRAS*, 416, 2130
- Tauris, T. M., & Savonije, G. J. 1999, *A&A*, 350, 928
- Tauris, T. M. & van den Heuvel E. P. J., 2006, in *Compact Stellar X-Ray Sources*, Eds., W. H G. Lewin, M. van der Klis (Cambridge: Cambridge University Press), 623
- Tauris, T. M., van den Heuvel, E. P. J., & Savonije, G. J. 2000, *ApJ*, 530, L93
- The Fermi LAT Collaboration, 2011, *Science*, 334, 1107
- Thorsett, S. E. & Chakrabarty, D. 1999, *ApJ*, 512, 288
- Timmes, F. X., Woosley, S. E., & Weaver, Thomas A. 1996, *ApJ*, 457, 834
- Ustyugova, G. V., Koleoba, A. V., Romanova, M. M., & Lovelace, R. V. E. 2006, *ApJ*, 646, 304
- van den Heuvel, E. P. J. & Taam, R. 1984, *Nature*, 309, 235
- van der Meer, A., Kaper, L., van Kerkwijk, M. H., Heemskerk, M. H. M., & van den Heuvel, E. P. J. 2007, *A&A*, 473, 523
- van der Sluys, M. V., Verbunt, F., & Pols, O. R. 2005, *A&A*, 440, 973
- van Paradijs, J. 1996, *ApJ*, 464, L139
- Verbunt, F. & Zwaan, C. 1981, *A&A*, 100, L7
- Wang, Y.-M. 1995, *ApJ*, 449, L153
- Webbink, R. F. 1984, *ApJ*, 277, 355
- Webbink, R. F., Rappaport, S. A., & Savonije, G. J. 1983, *ApJ*, 270, 678

Woosley, S. & Janka, T. 2005, *Nat. Phys.*, 1, 147

Zhang, C. M., Wang, J., Zhao, Y. H., Yin, H. X., & Song, L. M. et al. 2011, *A&A*, 527, A83

Zhang, Z. & Li, X.-D. 2010, *A&A*, 518, A19

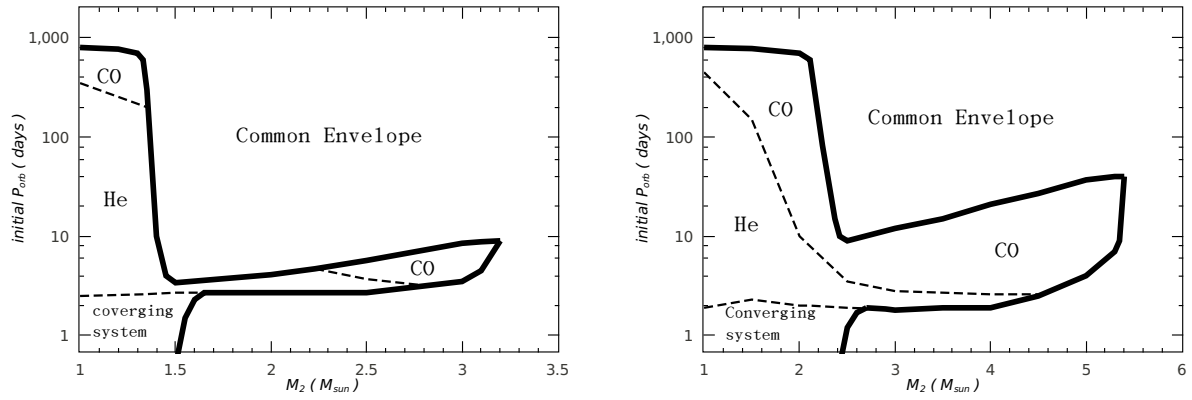


Fig. 1.— The thick lines confine the allowed parameter space in the initial orbital period vs. donor mass plane for I/LMXBs to successfully form binary pulsars with He and CO WD companions. In the left and right panels the initial mass of the NS is taken to be $1.0 M_{\odot}$ and $1.8 M_{\odot}$, respectively.

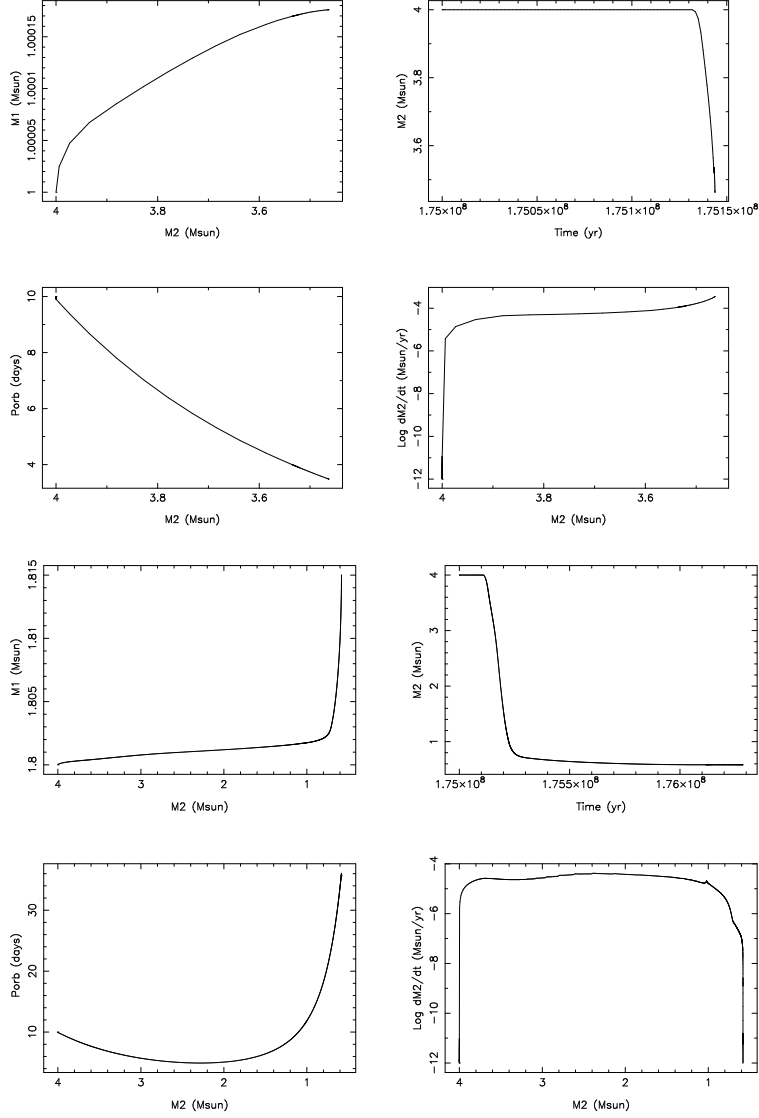


Fig. 2.— Evolution of the NS mass M_1 , the donor mass M_2 , the orbital period P_{orb} , and the mass transfer rate \dot{M}_2 for a IMXB consisting of a $1.0 M_{\odot}$ (upper two panels) or $1.8 M_{\odot}$ (lower two panels) NS.

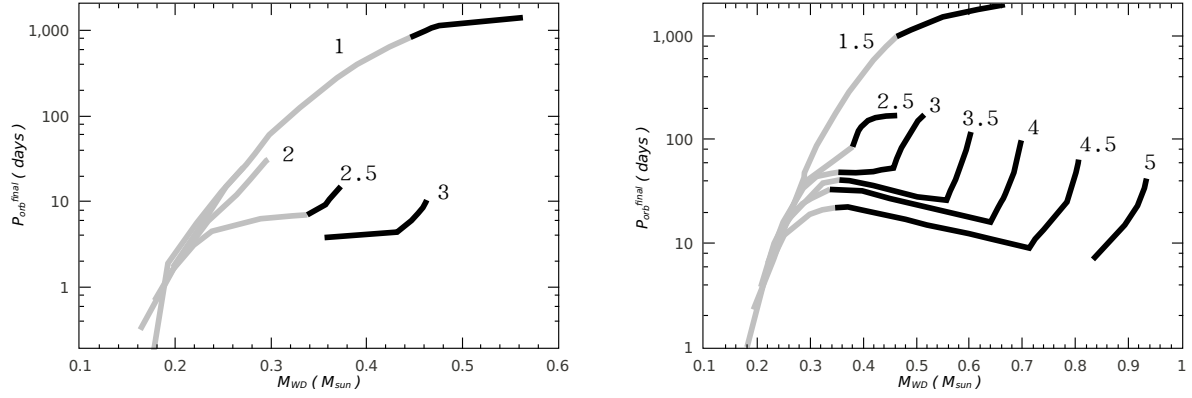


Fig. 3.— The final orbital period P_{orb} as a function of the WD mass M_{WD} for binary pulsars with an initial $1.0 M_{\odot}$ (left) or $1.8 M_{\odot}$ (right) NS. The number next to each curve denotes the initial mass of the donor star (the progenitor of the WD). The gray and black curves represent binary pulsars with He and CO WD companions, respectively.

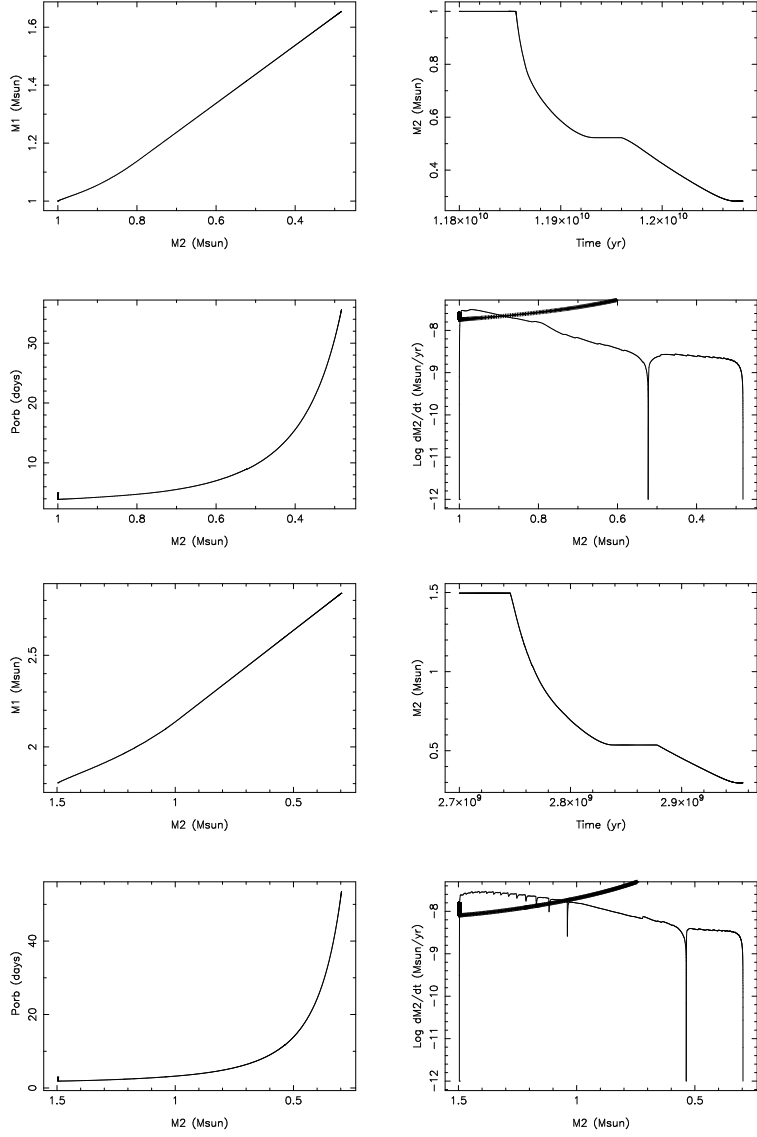


Fig. 4.— Evolution of the NS mass M_1 , the donor mass M_2 , the orbital period P_{orb} , and the mass transfer rate for a LMXB with a $1.0 M_{\odot}$ NS and a $1.0 M_{\odot}$ initial donor (upper two panels) or with a $1.8 M_{\odot}$ NS and a $1.5 M_{\odot}$ initial donor (lower two panels). The thick lines represent the critical mass transfer rate for unstable accretion disks.

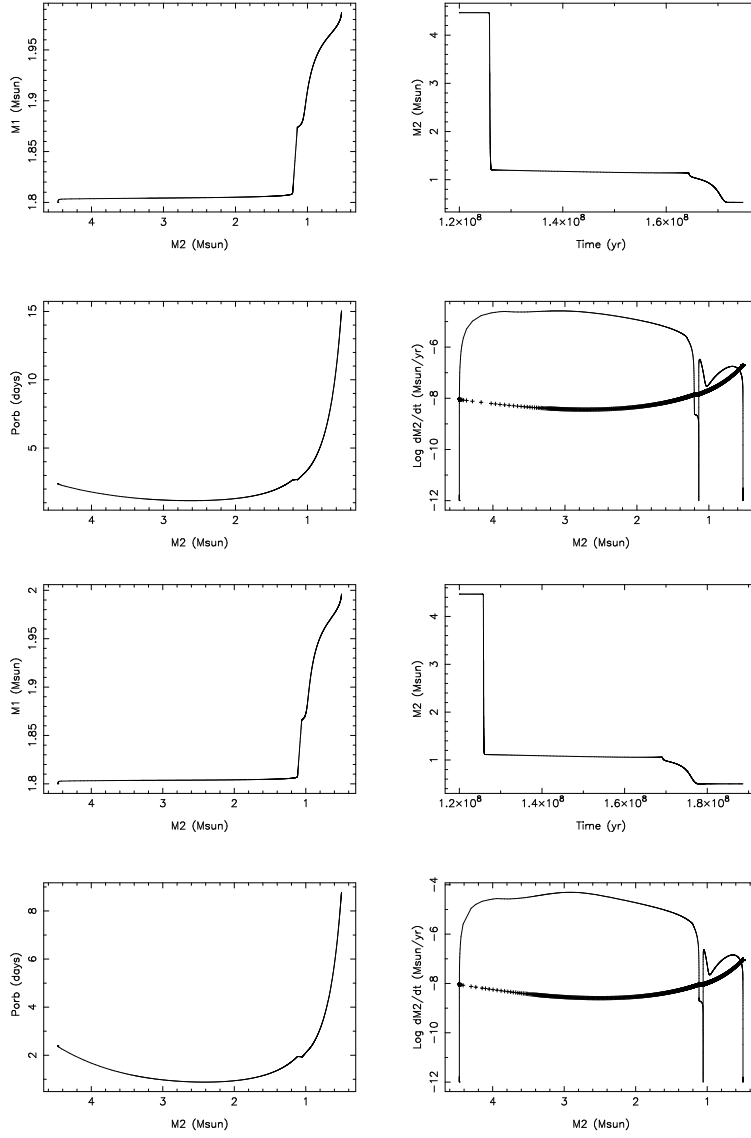


Fig. 5.— This figure shows the effect of outflow from the L_2 point on the formation of MSP J1614–2230. The upper two and lower two panels correspond to $\delta = 0$ and 0.04, respectively.

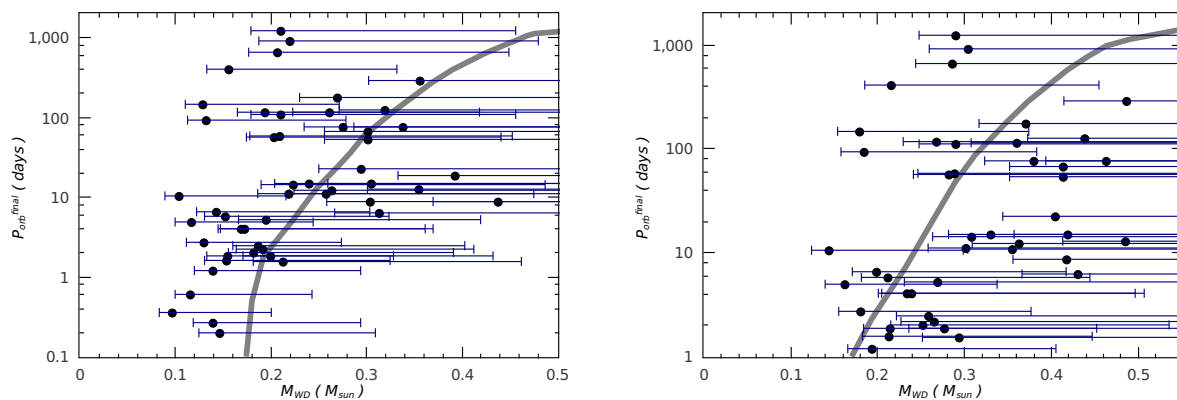


Fig. 6.— The orbital period as a function of the WD mass for MSPs with possible He WD companions. In the left and right panels the thick lines are theoretically expected relations for NSs with an initial mass of $1.0 M_{\odot}$ and $1.8 M_{\odot}$, and the dots correspond to binary pulsars with an assumed mass of $1.2 M_{\odot}$ and $2.0 M_{\odot}$, respectively. The error bars of the WD masses cover the 90% probability mass range for randomly oriented orbits having $i = 90^{\circ}$ to $i = 26^{\circ}$.

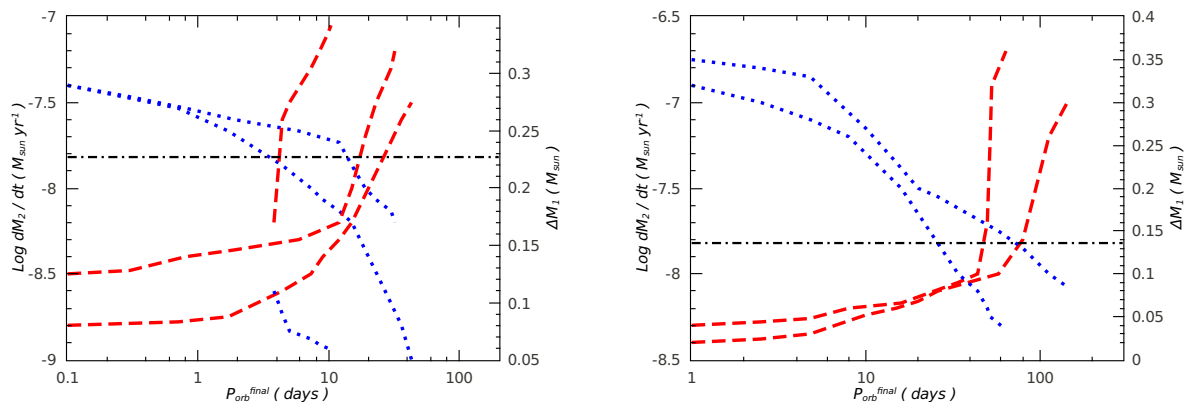


Fig. 7.— The mass transferred rate (red dashed curves) and accreted masses (blue dotted curves) of the NS as a function of the final orbital period for binaries with a $1.0 M_{\odot}$ (left panel) or $1.8 M_{\odot}$ (right panel) NS. The black dot-dashed line show the critical accretion rate \dot{M}_{Edd} . In the left panel, the red dashed (blue dotted) curves, from bottom (top) to top (bottom), correspond to 1.0 , 2.0 , and $3.0 M_{\odot}$ donor stars, respectively. In the right panel, plotted are those in the cases of 2.0 and $3.0 M_{\odot}$ donor stars.

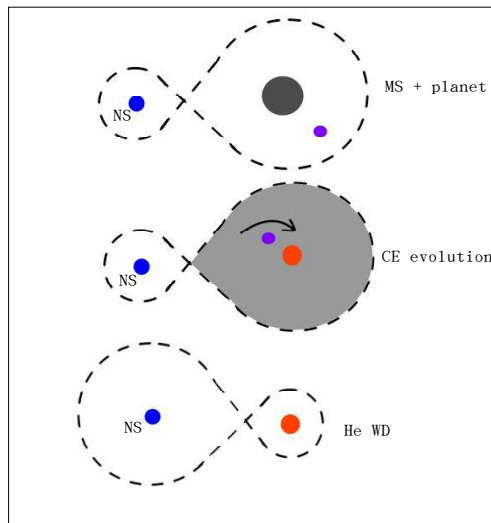


Fig. 8.— This schematic plot shows the possible formation process of wide BMSPs with a He WD companion. We assume that in a wide binary (with orbital period at least longer than tens of days) the secondary star initially possesses a (or multiple) substellar object(s), which spirals into the stellar envelope when it expands and develops a He core. The CE evolution may also cause the secondary to fill its Roche-lobe, and transfer mass rapidly to the NS. After the envelope is expelled, a wide binary with a NS and a He WD is produced. If the NS can accrete sufficient mass from its companion, it will appear as a MSP.

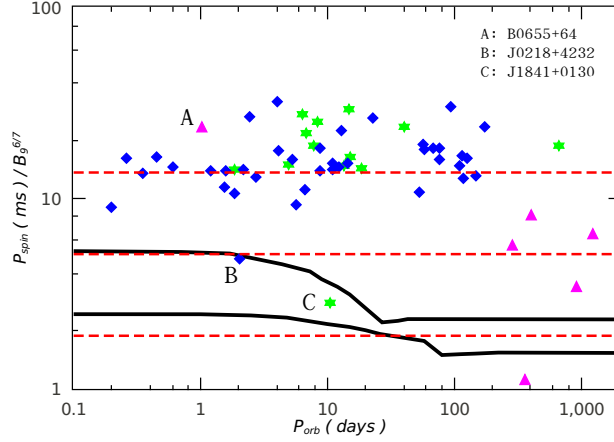


Fig. 9.— The black lines show the relationship between $P_{\text{eq}}/B_9^{6/7}$ and P_{orb} for all systems from our calculations. Blue diamonds, green stars, and magenta triangles represent binary pulsars with $P_{\text{spin}} \leq 10$ ms, $10 \text{ ms} < P_{\text{spin}} \leq 100$ ms, and $P_{\text{spin}} > 100$ ms, respectively. The red dashed lines from top to bottom correspond to mass accretion rate of 0.01, 0.1, and $1.0\dot{M}_{\text{Edd}}$ for a $1.4M_{\odot}$ NS, respectively.

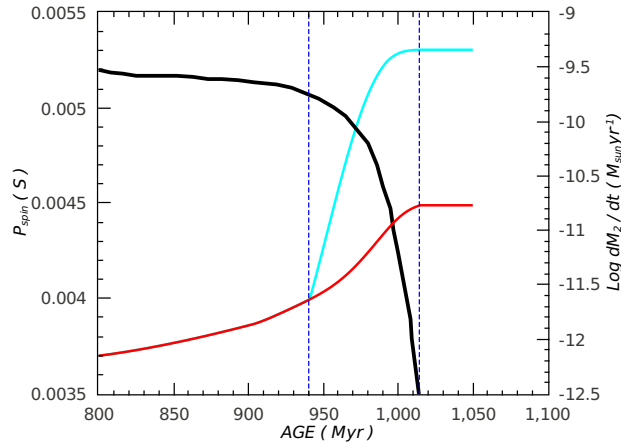


Fig. 10.— Spin evolution of an accreting NS at the end of mass transfer phase as in Tauris (2012). The black line denotes the evolution of the mass transfer rate, and the blue and red lines denote the spin evolution governed by Eqs. (11) and (12), respectively. The two vertical dashed lines confine the propeller phase.

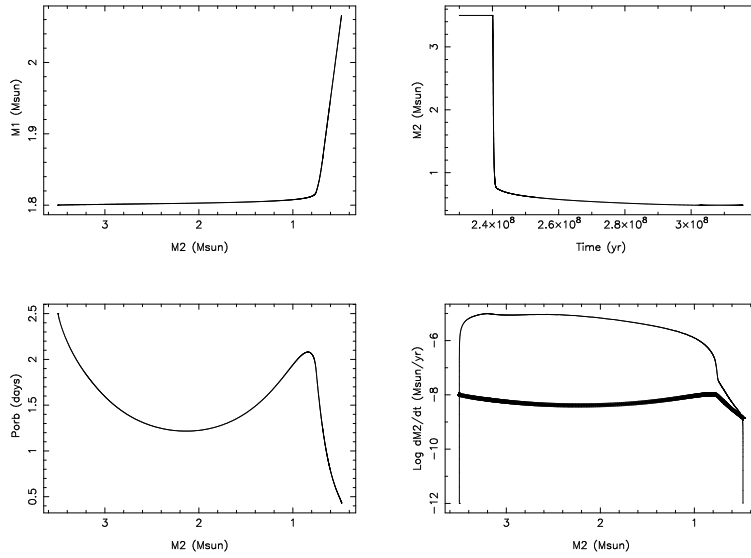


Fig. 11.— The evolution of the NS mass, the donor mass, the orbital period, and the mass transfer rate for a 1.8 M_{\odot} NS IMXB. With anomalous MB, the final outcome is a IMBP with orbital less than 1 d. The thick line corresponds to the critical mass transfer rate for unstable accretion disks.

Table 1: Parameters of Intermediate-Mass Binary Pulsars with $P_{\text{orb}} \lesssim 1$ d^a

Pulsar	P_{spin} (ms)	P_{orb} (d)	M_{WD}^b	B (G)
B0655+64	195.6	1.0287	0.80	1.17×10^{10}
J1435–6100	9.3	1.3549	1.08	4.84×10^8
J1757–5322	8.9	0.4533	0.67	4.89×10^8
J1802–2124	12.6	0.6989	0.98	9.69×10^8
J1952+2630	20.7	0.3919	1.13	

^aData are taken from the ATNF pulsar catalogue.

^bMedian mass for the inclination angle $i = 60^\circ$.